# Design of Jitter-Robust Orthogonal Pulses for UWB Systems

Giuseppe Thadeu Freitas de Abreu and Ryuji Kohno

*Abstract*— **The design of a class of Hermite pulses for Pulse Shape Modulated (PSM) Ultra-Wideband (UWB) communications is presented. The proposed pulses offer robustness against jitter or small imperfections in synchronization between received waveforms and their matched templates. Close form expressions of the auto- and cross-correlation functions of the proposed and conventional Hermite pulses are given, which are used to model the jitter channel as a simple distortive matrix. The set of jitter-robust orthogonal pulses is then obtained by simultaneously diagonalizing a subset of selected samples of such channel matrix realizations for different jitter values. Examples of waveforms derived with the method and Simulation results showing the effectiveness of the proposed pulses in combatting jitter in PSM-UWB systems are given.**

## I. INTRODUCTION

Pulse-Shape Modulated (PSM) with orthogonal Hermite pulses have been proposed as an alternative to conventional Pulse-Position Modulated (PPM) for Ultra-Wideband (UWB) communications by [1]. Developing on that idea, it has been shown [2] that two-dimensional modulation schemes can be designed for UWB systems, with direct implication on achievable capacity.

Hermite pulses form an orthonormal basis that can be used to derive finite sets of waveforms optimized to meet a specific design goals. For instance, in [3], Hermite pulses are combined to obtain a set of orthogonal waveforms with similar spectra and no DC components.

In this paper, a similar approach is taken to address the presence of jitter in the UWB cannel. Typical values of root mean square (rms) jitter in PPM-UWB systems range from a few to several tens of picoseconds [4].

It was also shown in [4] that jitter can significantly reduce the performance of a PPM-UWB system with a Time-Hopping (TH) multiple access scheme. In PSM-UWB systems, the degradation is more critical since the orthogonality of conventional Hermite pulses is destroyed by jitter. In order to solve this problem, we propose a method to design a class of jitter-robust Hermite-based waveforms for PSM-UWB communications.

## II. HERMITE DECOMPOSITION AND THE JITTER CHANNEL

### A. Hermite Decomposition

Let the Hermite polynomial of order $n$ be defined in the interval $(-\infty, \infty)$ by the Rodrigues formula as follows [5]:

$$H_n(t) \equiv (-1)^n e^{t^2} \frac{d^n}{dt^n} e^{-t^2} \quad n \in \mathbb{N}. \tag{1}$$

Orthogonal Hermite pulses may then defined by [3]

$$\psi_n(t) \equiv P_n e^{\frac{-t^2}{2}} H_n(t), \tag{2}$$

where $P_n$ is a factor that normalizes the energy of $\psi_n(t)$.

This normalization coefficient is obtained from the orthogonality property of Hermite polynomials [5] given by

$$\int_{-\infty}^{\infty} e^{-t^2} H_n(t) H_m(t) dt = \begin{cases} 0 & \text{if} \quad n \neq m \\ 2^n n! \sqrt{\pi} & \text{if} \quad n = m \end{cases}, \tag{3}$$

which, in turn, gives

$$P_n = \frac{1}{\sqrt{2^n n! \sqrt{\pi}}}. \tag{4}$$

Combining the definition (2) and equation (4) we obtain:

$$\int_{-\infty}^{\infty} \psi_n(t) \psi_m(t) dt = \delta(n, m) \tag{5}$$

where $\delta(n, m)$ is the Kronecker delta.

It is clear from (5) that Hermite pulses form an orthonormal basis of a space which we henceforth refer to as the *Hermite Space* (as opposed to Hermite space usually defined over Hermite polynomials) [5]. Invoking the fact that shifted pulses are smooth functions of $t$ and assuming that the random jitter values $\tau$ are enough smaller than the pulse width, an jitter-shifted pulse $\psi_n(t-\tau)$ can be decomposed in a Hermite series. For an $N$ dimensional space we have:

$$\psi_n(t - \tau) \approx \sum_{k=0}^{N-1} c_{k,n}(\tau) \psi_k(t). \tag{6}$$

Note that the coefficients $c_{k,n}(\tau)$ are nothing but the cross-correlation between the jitter-shifted $n$-th order pulse and the $k$-th order elementary Hermite pulse centered at $t = 0$. Indeed, multiplying equation (6) by $\psi_m(t - \tau)$, integrating over the interval $(-\infty, \infty)$ and making use of the pulse orthogonality property given in (5) we have

$$c_{m,n}(\tau) = \int_{-\infty}^{\infty} \psi_m(t) \psi_n(t - \tau) dt. \tag{7}$$

This integral has the close form expression given in equation (8) at the top of the next page.

Generally, the larger the order and the delay of the decomposed pulse relative to the basis of the Hermite space, the larger the dimension $N$ required for an accurate truncated series representation.

 0-7803-7974-8/03/$17.00 

$$c_{m,n}(\tau) = \begin{cases} \frac{(-1)^{2m+n}\tau^{n+m}\sqrt{n!m!}}{\sqrt{2^{n+m}}} e^{-\frac{\tau^2}{4}} \sum_{k=0}^{min(n,m)} \frac{(-1)^k \tau^{-2k}\sqrt{4^k}}{(n-k)!(m-k)!k!} & \text{if} \quad m \neq n \\ 1 & \text{if} \quad m = n \end{cases} \tag{8}$$

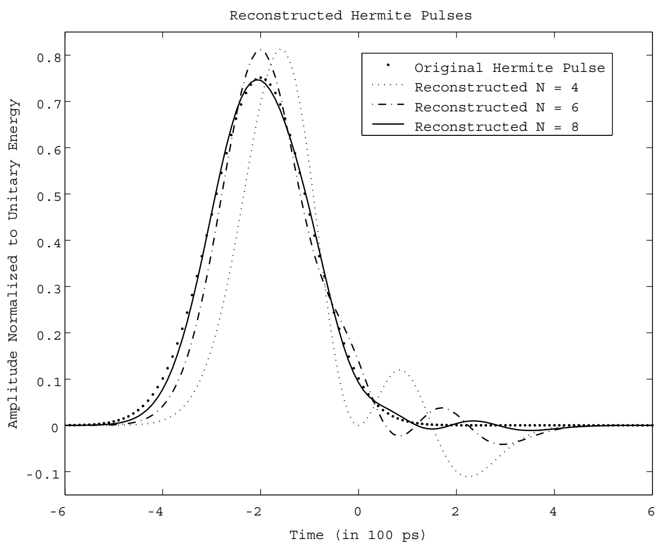


Fig. 1. Reconstruction of a delayed 0-th order Hermite pulse

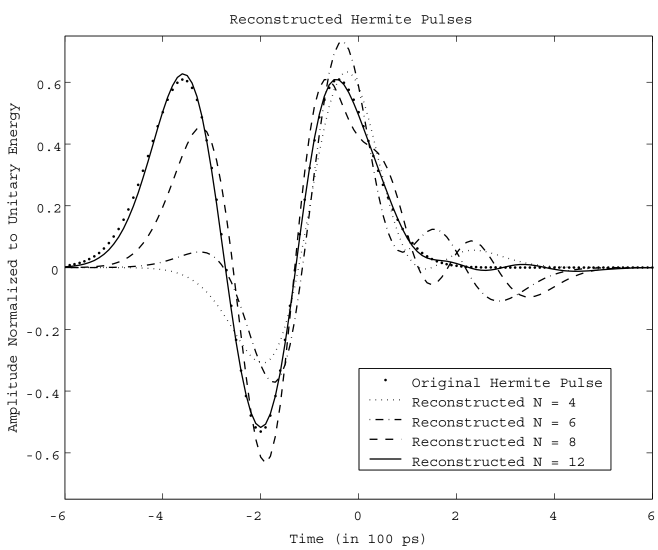


Fig. 2. Reconstruction of a delayed 2nd order Hermite pulse

Figures 1 and 1 illustrate this by showing the results obtained by reconstructing the 0-th and 2nd order Hermite pulses, delayed by 200 picoseconds, using different numbers of elementary Hermite pulses.

### *B. Jitter Channel Model*

A noiseless delay channel is often described by convolutional unitary impulse response channel [6], *i.e.*, the signal $s(t)$ delayed by an amount $\tau$ is modelled by

$$s(t-\tau) = s(t) * \delta(t-\tau) = \int_{-\infty}^{\infty} s(x)\delta(x-\tau)dx \tag{9}$$

where $*$ denotes the convolution and $\delta(t)$ is the unitary impulse at $t = 0$. The difficulties in adequately applying signal processing techniques developed under such a model in UWB systems are evident, given the extremely short duration of pulses. On the other hand, a direct consequence of the application of Hermite decomposition to analyze delayed Hermite pulses is that, since $c_{m,n}(\tau)$ are known for all $\tau$, $m$ and $n$, a theoretical, multiplicative model of the jitter channel can be easily derived.

Indeed, using (8), the jitter channel can be modelled by an $N$-by-$N$ matrix $\mathbf{A}(\tau)$ defined as

$$\mathbf{A}(\tau) = \begin{bmatrix} c_{0,0}(\tau) & c_{0,1}(\tau) & \cdots & c_{0,N-1}(\tau) \\ c_{1,0}(\tau) & c_{1,1}(\tau) & \cdots & c_{1,N-1}(\tau) \\ \vdots & \vdots & \ddots & \vdots \\ c_{N-1,0}(\tau) & c_{N-1,1}(\tau) & \cdots & c_{N-1,N-1}(\tau) \end{bmatrix}, \tag{10}$$

where $\tau$ is a Gaussian random with zero-mean and variance $\sigma_\tau^2$.

Therefore, using $\mathbf{A}(\tau)$, a received waveform with a given delay $\tau$ relative to the receiver templates, can be represented as a weighted sum of non-delayed elementary Hermite pulses.

Let the vector representation of the $n$-th order pulse be

$$\overrightarrow{\psi_n} = [\delta_{k,n}]_{\ k=0,\ldots,N-1}\ , \tag{11}$$

where $\delta_{k,n}$ is the Kronecker delta defined by

$$\delta_{k,n} = \begin{cases} 1 & \text{if} \quad n = k \\ 0 & \text{if} \quad n \neq k \end{cases} . \tag{12}$$

Then, the vector representation of the receive waveform corresponding to the $n$-th order transmit pulse delayed by $\tau$ is

$$\overrightarrow{\psi_n}\Big|_\tau \approx \sum_{k=0}^{N} c_{k,n}(\tau)\overrightarrow{\psi_k} = \mathbf{A}(\tau)\overrightarrow{\psi_n}. \tag{13}$$

Next, let the set of vector representations of all individual $N-1$ Hermite pulses available at the transmitter be denoted by $\overrightarrow{\mathbf{\Psi}} = \left\{\overrightarrow{\psi_n}\,|n = 0,\ldots,N-1\right\}$. At each transmit interval, a subset $\overrightarrow{\mathbf{\Phi}} \subseteq \overrightarrow{\mathbf{\Psi}}$ of these pulses may be simultaneously transmitted. The resulting waveform is represented by the sum of all vectors in $\overrightarrow{\mathbf{\Phi}}$ and is denoted $\overrightarrow{\phi}$. From the linearity of (13), the corresponding receive waveform is simply

$$\overrightarrow{\phi}\Big|_\tau = \mathbf{A}(\tau)\overrightarrow{\phi}. \tag{14}$$

Studying (8) we have noticed that, for small values of $\tau$, $\mathbf{A}(\tau)$ are *quasi*-commutative matrices with real entries.

In the next section this property is invoked to design a set of orthogonal pulses with robustness against jitter, based on the combination of conventional Hermite pulses.

## III. Design of Jitter-Robust Pulses

If $\tau$ is small enough that the Hermite decomposition defined by equations (6) and (8) is applicable, then the matrices $\mathbf{A}(\tau)$ given in (10) are all real and contain no zeros along its main diagonal. In addition, since all elementary pulses $\psi_n(t)$ are orthogonal, as demonstrates equation (5), the rows $\mathbf{A}(\tau)$ are linearly independent.

Typical values of $\sigma\tau$ for UWB systems are from 10 to 150 picoseconds, while pulses are about 1 nanoseconds in duration [4]. Therefore, for practical purposes, $\mathbf{A}(\tau)$ are positive definite.

It is easy to verify through simulations that the matrices $\mathbf{A}(\tau)$ are nearly commutative, *i.e.*, $\mathbf{A}(\tau_1) \approx \mathbf{A}(\tau_2)$, especially for large $N$ and small $\tau$. On the other hand, it has been shown in [7] that nearly commutative matrices can be jointly diagonalized using a Jabobi-like iterative algorithm. Details on the algorithm as well as a thorough investigation on its properties, convergency and robustness to round-error perturbations are given in [7], and therefore are omitted in this paper.

Among the important results reported in [7] is the fact that the Jacobi-like iterative algorithm works well with non-strictly commutative matrices, as opposed to the simpler version fount in [8]. In fact, it was also shown in [9] that the Jacobi angles iteratively computed to solve the constrained minimization problem to which the simultaneous diagonalization problem reduces to, has a close form valid for any set of $N$-by-$N$ matrices, commuting or not, real or not. Furthermore, a simplified algorithm exists for the case of matrices of real entries was given in [9]. Therefore, we establish the following design procedure for the design of Hermite-based orthogonal waveforms for PSM-UWB communications.

First, construct the set $\mathcal{A}_K = \{\mathbf{A}(\tau_k)\,|k = 0, 1, \ldots, K\}$ of $K$ Hermite decomposed matrices. Since each $\mathbf{A}(\tau_k)$ models a channel with delay $\tau_k$, we refer to $\mathcal{A}_K$ as the set of $K$ *channel samples*.

It is natural to choose these samples based on the Probability Density Function (PDF) of the random $\tau$. Let $P(\tau_{k-1} \leqslant \tau < \tau_k)$ denote the probability that $\tau$ is between $\tau_{k-1}$ and $\tau_k$. Then, given a jitter variance $\sigma_\tau^2$ we determine each $\tau_k$ such that

$$P(\tau_{k-1} \leqslant \tau < \tau_k) = P(\tau_k \leqslant \tau < \tau_{k+1}), \tag{15}$$

where

$$P(\tau_{k-1} \leqslant \tau < \tau_k) = \int_{-\tau_{k-1}}^{\tau_k} \frac{1}{\sqrt{2\pi}\sigma_\tau} e^{-\frac{\tau^2}{2\sigma_\tau^2}} d\tau. \tag{16}$$

Note that due to the symmetry of the PDF of $\tau$, it suffices to consider only positive values of $\tau_k$.

Next, we apply the theory of simultaneous diagonalization from [7] and [9], over $\mathcal{A}_K$ and obtain an orthogonal, $N$-by-$N$ matrix $\mathbf{X}$ that approximately diagonalizes, simultaneously, all matrices in a set. Mathematically we have

$$\exists\, \mathbf{X} \in \mathbb{R}^{n\times n} \left|\; \begin{array}{l} (1)\ \mathbf{X}^{\mathrm{T}}\mathbf{X} = \mathbf{I} \\ (2)\ \mathbf{X}^{\mathrm{T}}\mathbf{A}(\tau_k)\mathbf{X} \approx \mathbf{D}_k \;\forall\, k = 0, 1, \ldots, K \end{array}\right. \tag{17}$$

Then, take the $n$-th column of $\mathbf{X}$ – denoted by $\overrightarrow{x_n}$ – as the vector representation of a combination of Hermite pulses. The $n$-th order proposed pulse $\phi_n(t)$ is defined as the waveform composed by the sum of elementary Hermite pulses using the entries of $\overrightarrow{x_n}$. Thus

$$\phi_n(t) = Q_n \sum_{k=0}^{N-1} x_{k,n}\psi_k(t), \tag{18}$$

where $Q_n$ is a normalization computed from

$$\int_{-\infty}^{\infty} \left( \sum_{k=0}^{N-1} x_{k,n}\psi_k(t) \right)^2 dt = \sum_{k=0}^{N-1} (x_{k,n})^2, \tag{19}$$

which gives $Q_n = \dfrac{1}{\sqrt{\sum_{k=0}^{N-1} (x_{k,n})^2}}$.

Close form expressions for the cross-correlation between the proposed pulses can be easily derived from (7) and (8) giving

$$\int_{-\infty}^{\infty} \left( \sum_{i=0}^{N-1} x_{i,n}\psi_i(t) \right) \times \left( \sum_{j=0}^{N-1} x_{j,m}\psi_j(t-\tau) \right) dt = \sum_{k=0}^{N-1} \left( x_{k,n} \sum_{j=0}^{N-1} x_{j,m} c_{i,j}(\tau) \right) \tag{20}$$

which finally results in

$$\begin{aligned} d_{m,n}(\tau) &= \int_{-\infty}^{\infty} \phi_m(t)\phi_n(t-\tau)dt = \\ &= \frac{\sum_{i=0}^{N-1} \left( x_{i,n} \sum_{j=0}^{N-1} x_{j,m} c_{i,j}(\tau) \right)}{\sqrt{\sum_{k=0}^{N-1} (x_{i,n})^2}\sqrt{\sum_{j=0}^{N-1} (x_{i,m})^2}}. \end{aligned} \tag{21}$$

From equation (17) it is clear that $\overrightarrow{x_n}$ are nearly invariant to all $\mathbf{A}(\tau_k)$ simultaneously, that is,

$$\mathbf{A}(\tau_k)\overrightarrow{x_n} \approx \rho_k \overrightarrow{x_n} \;\forall\, \tau_k, n \tag{22}$$

where $\rho_k$ is a different constant for each $\tau_k$.

Therefore, for all $\tau_k$ we have $c_{i,j}(\tau_k) \approx \rho_k \delta_{i,j}$, which substituted into (21) gives

$$\begin{aligned} d_{m,n}(\tau_k) &\approx \frac{\rho_k \sum_{i=0}^{N-1} \left( x_{i,n} \sum_{j=0}^{N-1} x_{j,m} \right)}{\sqrt{\sum_{i=0}^{N-1} (x_{i,n})^2}\sqrt{\sum_{j=0}^{N-1} (x_{k,m})^2}} \\ &\approx \begin{cases} \rho_k & \text{if} \quad n = m \\ 0 & \text{if} \quad n \neq m. \end{cases} \end{aligned} \tag{23}$$

Equation (23) implies that, theoretically, the proposed pulses are nearly orthogonal at all $\tau_k$. In practice, since the matrices in $\mathcal{A}_K$ are not strictly commutative, the solution $\mathbf{X}$ does not strictly diagonalize all matrices in $\mathcal{A}_K$. A good measure of how far a given $\mathbf{A}(\tau_k)$ is from a truly diagonal matrix is $||\mathbf{I} - \mathbf{D}_k||_{\mathrm{F}}$ [7], where $||\mathbf{M}||_{\mathrm{F}}$ denotes the Frobenius norm, given by

$$||\mathbf{M}||_{\mathrm{F}} = \sqrt{\mathrm{trace}\,(\mathbf{M}^{\mathrm{H}}\mathbf{M})}. \tag{24}$$

Naturally, the pair $(\mathbf{A}(\tau_i), \mathbf{A}(\tau_j))$ is closer to a strictly commutative pair the closer $\tau_i$ and $\tau_j$ are. Since the PDF of $\tau$ is Gaussian, and given the criterion for choosing $\tau_k$ given in (15), we obviously have $\tau_k - \tau_{k-1} < \tau_{k+1} - \tau_k$. Consequently, we find that $||\mathbf{I} - \mathbf{D}_k||_{\mathrm{F}} < ||\mathbf{I} - \mathbf{D}_{k+1}||_{\mathrm{F}}$ for all $k$, with $||\mathbf{I} - \mathbf{D}_0||_{\mathrm{F}} \equiv \mathbf{0}$ since $\mathbf{A}(0) = \mathbf{I}$. In other words, the proposed pulses are strictly orthogonal at $\tau = 0$ and exhibit, although not strict orthogonality, lower cross-correlation in its vicinity.

Since the accuracy of the Hermite decomposition onto a Hermite space of finite dimension decreases with the order of the decomposed pulse, as shown in figures 1 and 2, it is expected that the robustness against jitter reduces with the pulse order. Therefore, in order to design a set of $K$ pulses with similar robustness against jitter, $N > K$ of elementary Hermites are needed.

In the next section, simulation results illustrate key properties of the proposed set of pulses and demonstrate the advantage of its usage in PSM-UWB systems, as compared to conventional PSM-UWB systems [10].

## IV. Simulations

In figure 3, a few waveforms obtained with the proposed method are compared against those of conventional Hermite pulses [1] for $N = 8$. Note that, since the proposed waveforms are combinations of $N$ elementary Hermites, the widths of pulses of different orders are nearly the same, as opposed to what is observed with conventional Hermite pulses.

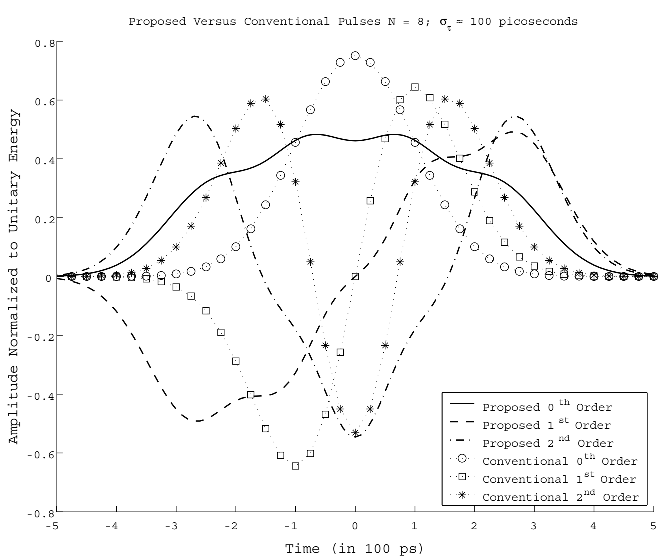


Fig. 3. Proposed Waveforms versus Conventional Hermite Pulses

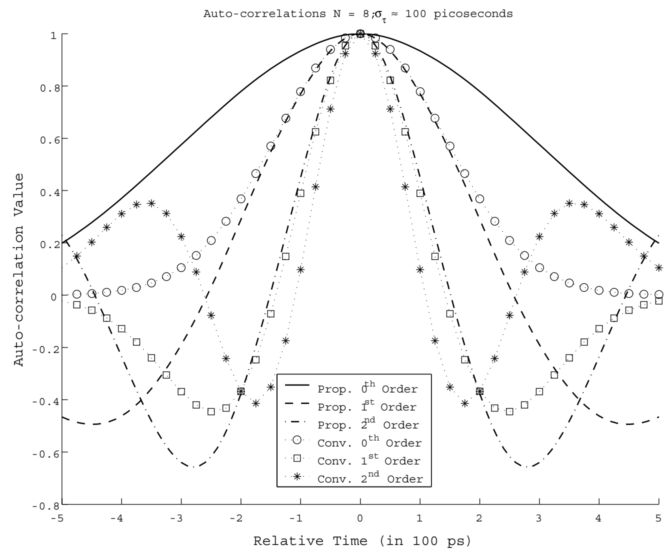


Fig. 4. Autocorrelation functions of proposed and conventional pulses ($N$=8)

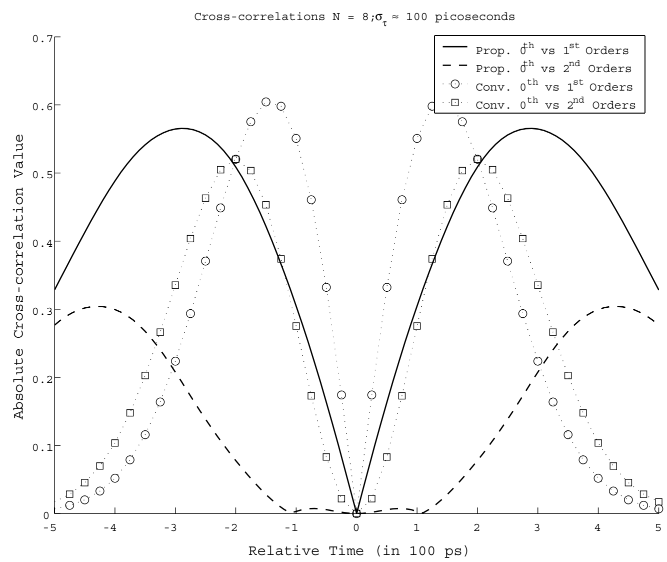


Fig. 5. Crosscorrelation functions of proposed and conventional pulses ($N$=8)

The auto and cross-correlation functions of the waveforms shown in figure 3 are compared in figures 4 and 5.

Note that the auto-correlation functions of the proposed pulses have significantly wider lobes – and the cross-correlation values of the proposed waveforms remain lower – than those of conventional Hermites in the vicinity of $\tau = 0$. Ever better results are achieved larger the ratio $N/K$ between the dimension $N$ of the Hermite space used and the highest order $K$ of the pulses designed.

Using the proposed waveforms results in lower probabilities of error than using conventional Hermites in a channel with jitter and Additive White Gaussian Noise (AWGN). This is confirmed in figures 6 and 7, where Symbol Error Rate (SER) curves for a binary PSM-UWB system using the two types of pulses are compared, for the cases when $\sigma_\tau^2 = 10,\ 30$and 50ps and Hermite spaces of size $N = 8$ and $N = 16$.

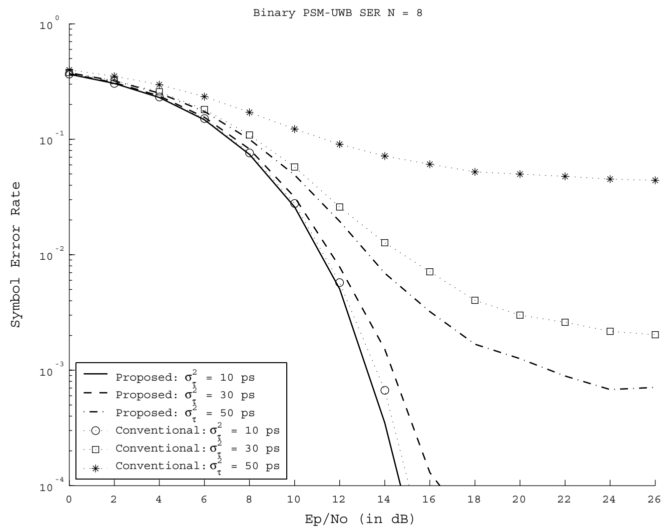


Fig. 6. Symbol Error Rates of Binary PSM-UWB with Proposed and Conventional Pulses ($N = 8$)

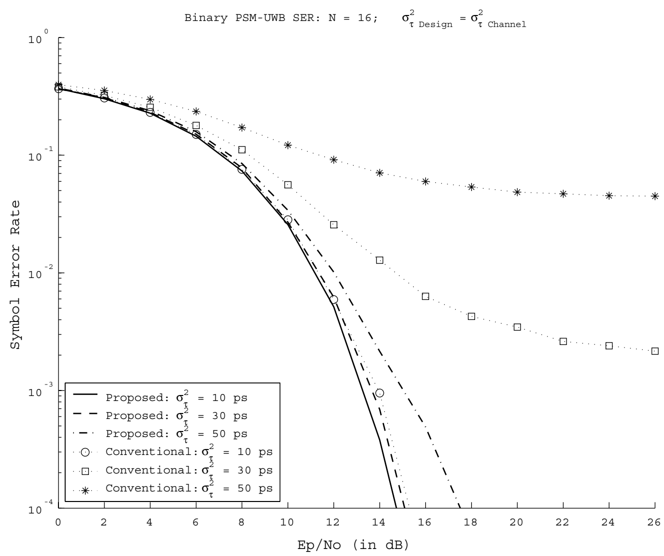


Fig. 7. Symbol Error Rates of Binary PSM-UWB with Proposed and Conventional Pulses ($N = 16$)

Although UWB systems usually require several pulses per symbol transmission [11], only the relative performances with the two pulses sets is of interest here and, therefore, the systems analyzed are all one-pulse-per-symbol PSM-UWB.

From the plots it is observed that, generally, a higher jitter variance results in a worse performance. However, PSM-UWB systems with the waveforms derived with the proposed design always outperform their equivalent with conventional Hermites. In fact, a binary one-pulse-per-bit system with the proposed pulses constructed with $N = 8$, sustains the SER of $10^{-3}$ at Ep/No=15 dB in a channel with 30 ps rms jitter.

This gain increases when the size of the Hermite space used in the design is larger. For instance, with $N = 8$, both the binary PSM-UWB system with the proposed waveforms and with conventional Hermites reach an error floors in the order of $10^{-4}$ in a channel with an rms jitter of 50 picoseconds.

With $N = 16$, however, no error floor is observed with the the binary PSM-UWB system using the proposed waveforms in the same channel.

## V. Conclusions

The design of jitter-robust waveforms for PSM-UWB communications was presented. A Hermite decomposition is used to model the jitter channel with a family $\mathcal{A}_\infty$ of $N$-by-$N$ real, *quasi*-commutative matrices with accuracy increasing in direct proportion to $N$ and inverse proportion to $\tau$. A Jacobi-like algorithm for simultaneous approximate diagonalization of such matrices is applied over a set $\mathcal{A}_K$ of selected samples of $\mathcal{A}_\infty$.

The solution $\mathbf{X}$ of this generalized eigen-problem yields the coefficients used to combine elementary Hermites and design the desired set of orthogonal, jitter-robust pulses.

Simulations confirming the enhanced properties of the proposed pulses relative to conventional Hermites, and their advantageous application in PSM-UWB systems in the presence of jitter and AWGN were given.

In this work, the effects of distortions that can affect the shape of UWB pulses were not taken into account. One of these effects is differentiation introduced by common resistive-capacitive antennas [12]. In a future work we shall extend the design here presented so as to take into account the effect of such distortions.

## References

[1] M. Ghavami, L. B. Michael, and R. Kohno, "Hermite function based orthogonal pulses for uwb communications," in *Proc. IEEE Wireless Personal Multimedia Conference (WPMC'01)*, Aalborg, Denmark, Sept. 2001, pp. 437–440.

[2] C. J. Mitchell, G. T. F. de Abreu, M. Hernandez, and R. Kohno, "A novel modulation design employing pulse shape and pulse position modulation for high data rate transmissions in uwb communications," *International Journal of Wireless Information Network - Special Issue on UWB (to appear)*, vol. 11, Apr. 2004.

[3] J. A. N. da Silva and M. L. R. de Campos, "Orthogonal pulse shape modulation for impulse radio," in *Proc. IEEE International Telecommunications Symposium (ITS'02)*, Natal, Brazil, Sept. 2002, pp. 916–921.

[4] W. M. Lovelace and J. K. Townsend, "The effects of timing jitter on the performance of impulse radio," *IEEE J. Select. Areas Commun.*, vol. 20, no. 9, pp. 1646–1651, Dec. 2002.

[5] A. D. Poularikas, *The Transforms and Applications Handbook, Second Edition*, 2nd ed. CRC Press, Feb.23 2000.

[6] J. G. Proakis, *Digital Communications, Fourth Edition*. New York, NY: Mc-Graw-Hill, 2000.

[7] A. B. Gerstner, R. Byers, and V. Mehrmann, "Numerical methods for simultaneous diagonalization," *SIAM Journal on Matrix Analysis and Applications*, vol. 14, no. 4, pp. 927–949, 1993.

[8] G. H. Golub and C. F. van Loan, *Matrix Computations*, 3rd ed. New York, NY: Johns Hopkins Univ Press, Nov. 1996.

[9] J.-F. Cardoso and A. Souloumiac, "Jacobi angles for simultaneous diagonalization," *SIAM Journal on Matrix Analysis and Applications*, vol. 17, no. 1, pp. 161–164, 1996.

[10] L. B. Michael, M. Ghavami, and R. Kohno, "Multiple pulse generator for pulses," in *Proc. IEEE Conference on Ultra Wideband Systems and Technologies*, Baltimore, U.S.A., May21-23 2002, pp. 47–51.

[11] M. Z. Win and R. A. Scholtz, "Impulse radio: How it works," *IEEE Commun. Lett.*, vol. 2, pp. 36–38, 1998.

[12] G. T. F. de Abreu, C. J. Mitchell, and R. Kohno, "On the design of orthogonal pulse-shape modulation for uwb systems using hermite pulses," *Journal of Communications and Networks - Special Issue on Ultra-Wideband Communications (to appear)*, vol. 5, no. 4, Dec. 2003.